Magnetic Properties of Nano Crystalline Nickel, Samariumdoped Zinc Ferrite

Vasant Naidu
Professor/ECE
Sethu Inst. of Tech.,
Pulloor – 626115,
Tamilnadu, India

S.K.A.Ahamed KanduSahib
Asso.Proff./ECE
Sethu Inst. of Tech.,
Pulloor – 626115,
Tamilnadu, India

M.SheikDawood
Asso.Proff./ECE
Sethu Inst.of Tech.,
Pulloor – 626115,
Tamilnadu, India

M.Suganthi
Professor/ECE
Thiagarajar College ofEngineering,
Madurai625 015,
Tamilnadu, India

ABSTRACT: Nano-particles of polycrystalline Zn Fe_2 O_4 are prepared using sol-gel method with Ni, and Sm. They are obtained as dried gel after the successful chemical reaction of their respective metal nitrate solutions in the midst of citric acid as catalyst. Synthesis of materials is confirmed using XRD from the report of single phase polycrystalline ferrite material.

The magnetic properties of Zn-ferrite ceramics Zn_{1-x-y} Ni_ySm_x Fe_2 O_4, (where x = 0.01, 0.012, 0.014, 0.016, y=0.001) were synthesized by sol gel auto combustion method. The structure and composition of Sm doped Zn-ferrite ceramics were analyzed and the nano size was confirmed by the SEM monographs. The VSM studies confirm the magnetic behaviour by analyzing the change in magnetic saturation and coercivity of these nano materials.

Keywords: *Ferrimagnetic materials; Nanomaterials; Magnetization, VSM, SEM.*

1. INTRODUCTION

Nano-Ferrites of Zn_{1-x-y} Ni_ySm_x Fe_2O_4 , have technological importance as they can play a role in the miniaturization process of several microwave components [1–2]. It has been known in literature [3–5] that the substitution of Zinc in the bulk ferrites enabled a substantial modification of electrical and magnetic properties. Nano-ferrites with Zinc substitution, synthesized using sol-gel method, are studied in the present work. The sol-gel technique of preparing nanoferrite has many significant advantages such as good stoichiometric control and for the production of ultrafine particle with narrow size distribution in relatively short processing time at lower temperature [5–8].Consequently the difference in nature of cation and its distribution in spinel as well as ionic states of the metal ions in A- and B-sites when studied using X-ray diffraction (XRD), Vibrating sample magnetometer (VSM) and Infrared spectra (FTIR) would provide a meaningful correlation of their structure and effective changes in the environs of ions.

2. EXPERIMENTAL PROCEDURE

2.1 Synthesis Technique

A set of ferrites Zn_{1-x-y} Ni_ySm_x Fe_2 O_4 is synthesized using sol-gel (auto-combustion) method. The required amount of metal nitrates and citric acid are taken so as to have a molar ratio of 1:1 and dissolved in 100 ml of deionized water.

A required amount of ammonia is added into the solution in order to adjust the pH value to about 7since base catalysts are employed in order to speed up thereaction.

Sol so formed is poured in a silica crucible and heated at 135 - C under constant stirring to condensate into a xerogel. Dried gel is formed. Finally in dehydration process the xero gel (dried gel) is obtained by heating the product to 100 –C temperature. Citric acid helps the homogenous distribution of the metal ions to get segregated from the solutions. The grain size of the nanoferrite is determined using Scherrer's equation.

Using the knowledge of site preference of the ions and the ionic size data of the respective ions, the cation distribution has been estimated theoretically using the formula proposed [9, 10] (bottom of the page). Where r_a and r_b are the radii of the ions present in A-and B-site, respectively, whereas r_o is the ionic radius of oxygen in the formula.

The experimental magnetic moment is calculated from the following formula [11].

$$\eta = \frac{[M_W * M_S]}{5585}$$

Where MW is the molecular weight of the sample and Ms is the saturation magnetization in emu/g.

2.2 XRD and EDX Studies

XRD studies were done by using PAN analytical X'per PRO and EDX studies were done on Genesis EDX to study the structure of the powder material and the presence of the elements.

2.3 FTIR Study

Infrared absorption spectra in the range of 3.5 ×104 m^{-1} to 5.8 ×104 m^{-1} were recorded at room temperature byusing SHIMADZU FTIR spectrum one spectrometer using KBr pellet method. The spectrum transmittance (%) against wave number (m^{-1}) is used for interpretation of the results.

2.4 SEM Studies

Micrographs of the sensor were recorded using a scanning electron microscope (HITACHI model S-3000H).

2.5 Magnetic Measurements

The Magnetic measurements were performed using the commercial vibrating sample magnetometer (VSM) Lakeshore (Model73009). Magnetic hysteresis loops were measured at room temperature with maximal applied magnetic fields up to 0.95T.

$$a = \frac{\left\{\left(\frac{r_a}{\sqrt{3}} + r_b + 2.0951r_o\right) + \left[\left(\frac{r_a}{\sqrt{3}} + r_b + 2.0951r_0\right)^2 - 1.866(1.33{r_a}^2 + 0.0675{r_0}^2 + 0.6r_a r_0)\right]^{\frac{1}{2}}\right\}}{1.106}$$

Magnetic field sweep rate was 5 Oe/s for all measurements, so that the measurement of hysteresis loops with maximum field of 0.989 T took about three hours. The samples prepared in powder form were fixed in paraffin in order to exclude the motion of powder in a measuring cap. The saturation magnetization, coercivity and remanent magnetization were found from hysteresis loops.

3.0 RESULTS AND DISCUSSION

3.1 SEM Analysis

Fig. 1,2,3,4 shows the microstructure of sintered specimen. Unsubstituted specimen (Fig.1) shows the presence of a monophasic homogeneous microstructure with an average grain size 0.42nm.Whereas, Sm-doped specimens' show a bi-phasic microstructure constituted of dark ferrite matrix grains and small whitish grain at the grain junction/boundary in Fig 2, 3, and 4. As proposed by Pradeep et, al [10] the rare earth ions occupy either the iron positions or go to the grain boundaries. However we have to exclude the probability that the rare earth ions occupy the A- site of Fe^{3+} ions. This is due to the fact that the tetrahedral sites are small to be occupied by the large rare earth ions which have large ionic radius.

Of course the probability of occupancy of the octahedral (B-site) by the rare earth ions will increase with decrease in the R ionic radius. This indicated whitish grains were of $SmFeO_3$. The amount of $SmFeO_3$ was maximum in x¼ 0.016composition.The grain size of matrix phase was maximum in x¼ 0.016 composition in Fig.4. Relatively lower grain size of ferrite matrix in x¼ 0.01 compositions may be due to the grain growth inhibition caused by $SmFeO_3$ in Fig.1.

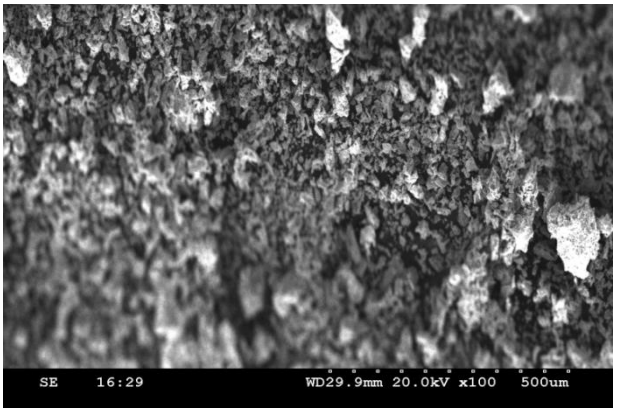

Fig.1 $Zn_{1-x-y}Ni_ySm_x Fe_2 O_4$ x=0.01, y=0.001

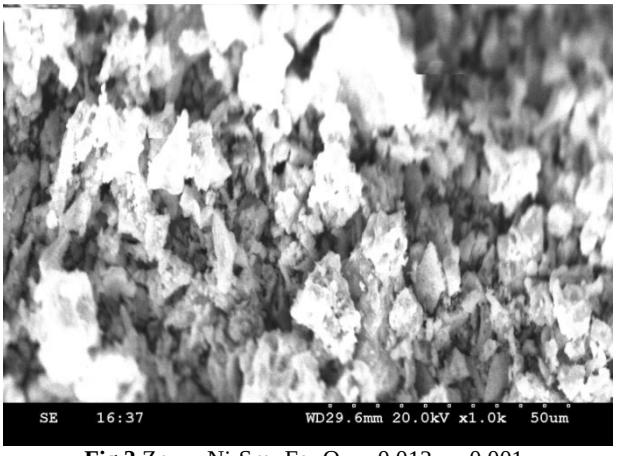

Fig.2 $Zn_{1-x-y}Ni_ySm_x Fe_2 O_4$ x=0.012, y=0.001

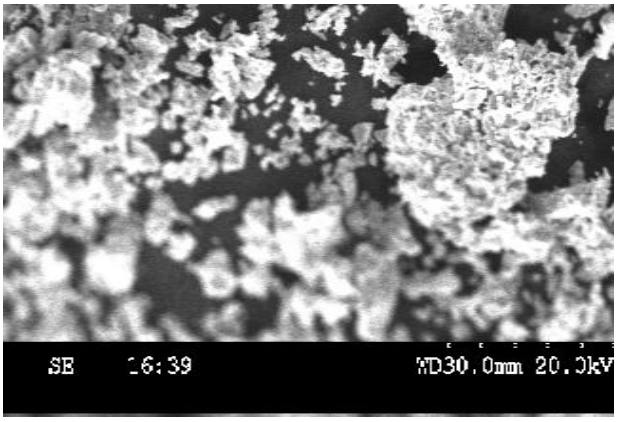

Fig.3 $Zn_{1-x-y}Ni_ySm_x Fe_2 O_4$ x=0.014, y=0.001

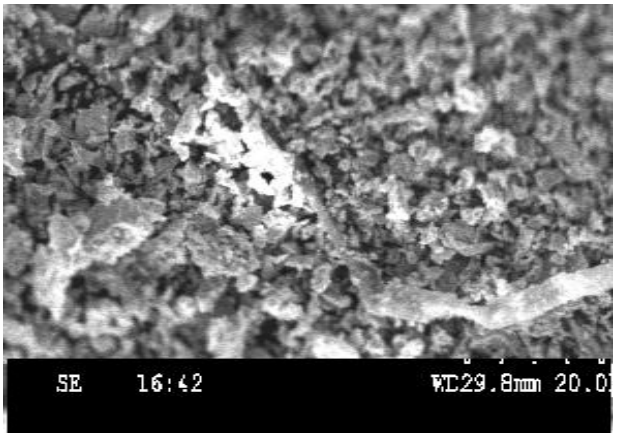

Fig.4 $Zn_{1-x-y}Ni_ySm_x Fe_2 O_4$ x=0.016, y=0.001

The grains in the unsubstituted sample are inhomogeneous i.e., the grains are affected by certain stress, while the grains for the Fe substituted sample are nearly homogeneous due to the decrease of stress. The photographs confirm these results that the stability increased for substituted samples.

3.2 Hysteresis Studies

Fig. 5 shows the variation in saturation magnetization (Ms) for the different x values of $Zn_{1-x-y}Ni_ySm_x Fe_2 O_4$ ferrite, the saturation magnetization (Ms) value increases within increase in the value of x. The Table 1 shows the theoretical calculation of magnetic moment of the ferrites is done after substituting the value of magnetic moment of the respective ion in the Neel's formula [11] as per the proposed cation distribution. Neel derived the well known'4/3' law for the dependence of coercivity on the film thickness t, $H_c \alpha\ t^{-4/3}$, which is valid under the assumption that the thickness fluctuation dt/dx, where dt/dx is the variation in the film thickness with position, (with x being the lateral direction along which the wall motion occurs) is constant.

$Zn_{1-x-y}Ni_ySm_xFe_2O_4$		Magnetic Saturation (emu)	Magnetic moment	Coercivity (G)	Retentivity (emu)
X=0.01	Y=0.001	0.0769	0.003331	392.9	0.0033
X=0.012	Y=0.001	0.1539	0.006671	147.0	0.0260
X=0.014	Y=0.001	0.2140	0.009283	124.0	0.0370
X=0.016	Y=0.001	0.2488	0.010800	155.0	0.0560

Calculation of the thickness dependence of the coercivity is performed by general expression as

$$H_c = Ct^n$$

Where t is a film thickness and c, n are fitting constant. The agreement of the theoretical and observed moment values as seen in Table3 supports the proposed cation distribution using XRD data. The observed values of magnetization and magnetic moment do not show agreement with the magnetic moment contribution of respective ions substituted in Znferrite i.e., Sm^{2+} and Ni^{2+} .However the coexistence of Fe^{2+} and Fe^{3+} ions in the octahedral site counterpoises disagreement which may be expected for room temperature condition. The magnetic moment for Ni substituted Zn ferrite is not in accordance with moment contribution of Ni^{2+} .This is observed to be so because of more number of Zn^{2+} ions than Ni^{2+} ions preferentially occupying the B-site in the case of Ni substituted Zn ferrite.

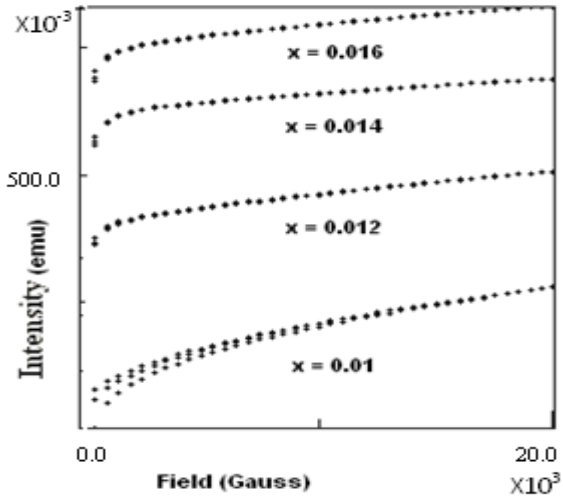

Fig.5 $Zn_{1-x-v}Ni_vSm_x Fe_2 O_4$ ferrites x=0.01,x=0.012, x=0.014, x=0.016 and y=0.001 Saturation magnetization (Ms)

The increasing samarium content induced a polar-to-nonpolar phase transition. Within the polar region, a rhombohedral and two orthorhombic modifications of $Zn_{1-x-v}Ni_vSm_x Fe_2 O_4$ were found. It was shown that samarium substitution resulted in the appearance of spontaneous magnetization, which was significantly enhanced upon the composition-driven transition from a rhombohedral to an orthorhombic phase.

3.3. FTIR Study

With a view to study the effect of dependence of normal modes and their frequency on change of the substitution of ions in Zn ferrite, FTIR frequency data for the respective sites are analyzed using the observed FTIR spectra shown in Fig.8. The higher frequency band (v_1) (555–565 cm^{-1}) and lower frequency band (v_2) (420–430 cm^{-1}) are assigned to the tetrahedral and octahedral complexes [12–13]. It explains that the normal mode of vibration of tetrahedral cluster is higher than that of octahedral cluster. It should be attributed to the shorter bond length of tetrahedral cluster and longer bond length of octahedral cluster. The values of bond lengths (R_A, R_B) and ionic size (r_A, r_B) of individual sites are obtained as a test of validity of interpretation from the experimental lattice constants of these ferrites. The values of force constant (K_A, K_B) have been calculated by substituting IR band frequency data in FG matrix formula [14].

The potential energy constant and magnetic moment data should provide information about the change of environs and energy conditions when Ni and Sm are substituted in Zn ferrite. Although the order of increase of ionic size is like Ni, Sm and Zn the values of magnetic moment Table 2 and force constant show a deviation for Ni substituted Zn ferrite. The deviations of ionic moment verses magnetic moment and bond length versus force constant of these ferrites are accounted for by a substantial role of crystal field effect [15] initiated by Zn ions.

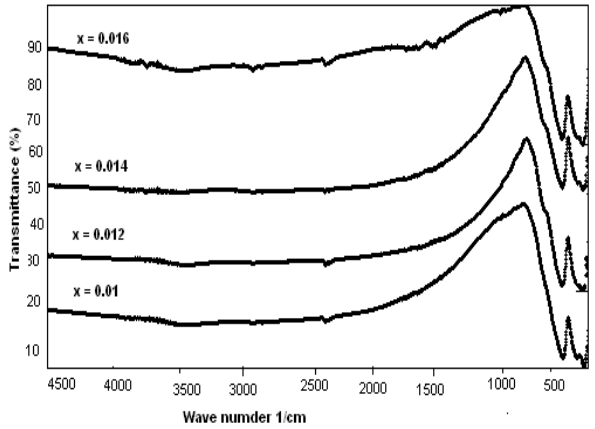

Fig.8FTIR spectra of nano-particles of $Zn_{1-x-v}Ni_vSm_x Fe_2 O_4$ Ferrite

Table 2. FTIR to show the rare-earth ions occupationin the B-site

Sample		Absorption/cm^{-1}	
		ν_1	ν_2
X=0.01	Y=0.001	372.25	349.09
X=0.012	Y=0.001	381.88	347.16
X=0.014	Y=0.001	385.74	362.59
X=0.016	Y=0.001	383.81	543.89

4.0 X-RAY DIFFRACTION

XRD patterns of sol-gel route-wise synthesized materials are shown in Fig. 12-15. The existence of a peak around the diffraction angle (2h) equal to 35- corresponding to (311) plane confirms the formationof spinel ferrites.

Table3 XRD cation distribution of $Zn_{1-x-v}Ni_vSm_x Fe_2 O_4$

Sample		Lattice Constant(A^o)	Particle Size(nm)
X=0.01	Y=0.001	8.41650	70.4054
X=0.012	Y=0.001	8.40001	79.3400
X=0.014	Y=0.001	8.40760	91.5116
X=0.016	Y=0.001	8.40460	96.7496

A careful analysis of XRD patterns helps to determine their respective planes and face centered cubic structure of these ferrites. Well resolved peaks in XRD pattern clearly indicate the single phase and polycrystalline nature of the samples. The values of lattice constant are determined for these materials and given in Table3.

It is found from Table 3 that Ni and Zn mixed ferrites have more values of lattice constant as they are bigger ions than Ni. Using the theoretical formula for lattice constant [16] the values of lattice constant have been calculated by a careful selection of cations in the octahedral and tetrahedral sites of ferrites so as to suit to the experimental lattice constants.

The proposed cation distribution is given in Table 3. The rules followed are: (i) A site has a sum of cationic distribution equal one and that for B site is considered as two and (ii)Zn has more preference to B site and B site is assumed to have Fe^{2+} ions. Using these conditions and the proposed distribution of cations provide one to one correspondence of theoretical and experimental lattice constants.

FWHM are taken from X-ray peak for (311) plane of the respective sample to estimate their particle size. The determination of particle size has been carried out using well known Scherrer'sformula . The values of particle size are given in Table 3. It is seen from Table 3 that the powder of synthesized ferrites is of nanocrystalline particles. The observed particle size decreases when ionic substitution moves as Ni and Sm i.e less the ionic size more will be size of the particles grown. The cause mechanism of this interesting feature is in the faster driving of the ions and consequent easier growth of particles when the ionic size is small during the synthesis.

It is well known that the degree of replacement of the host cations by the other ions in the host lattice depends on the cations radius of the substituent [17].

The lattice constant *a* (nm) of spinel structure could be calculated for prominent peak (311) using Bragg's equation[18].

$$a = d_{hkl}\sqrt{h^2 + k^2 + l^2}$$

Where hkl are the indices of mentioned planes.

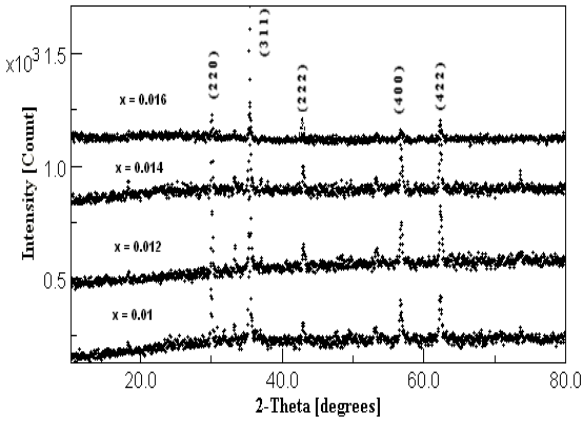

Fig.9 XRD patterns nano-particles of $Zn_{1-x-y}Ni_ySm_xFe_2O_4$ Ferrite

Lattice constants of all samples prepared in investigation are listed in Table 2. The lattice constant is smaller than pure $ZnFe_2O_4$ and increases with the increase in radius of Sm ions.

This is attributed to the large difference between cation radii of R^{3+} and Fe^{3+} owing to the removal of rare-earth ions from the spinel lattice. Similar behavior is also reported by Vermenko *et al.* [19] for Ni ferrite. The size of crystallite was evaluated by measuring the FWHM of the most intense peak (311) by the Debye Scherrer formula.

$$D = \frac{0.94\lambda}{\beta \cos\theta}$$

XRD patterns exhibit narrow reflection that points to the narrow size crystallites. The results are as shown in Table 3 the mean crystallite size of the sample lies in the range of 70.40 nm to 96.74 nm. The crystallite size of R ions added sample is smaller than pure Zinc Ferrite. This difference suggests that a diffusion inhibition induced by rare-earth ions during the formation of the mixed metal oxide. The mean crystallite size is lower than that reported by ceramic method.

4.1 EDX

The EDX spectra (Fig. 10 and Fig11) obtained from the center of grain boundary ZnFeO3 phase indicated the presence of mainly Zn, Fe and oxygen along with small amount of Sm, and Ni. The grain size of ferrite matrix phase as well as the $ZnFeO_3$ phase increased with increasing the La3+ substitutions. The EDX spectra (Fig. Fig. 10 and Fig11) obtained from the center of Zn substituted NiSm ferrite grains indicated the presence of small concentration of Zn inside the grains.

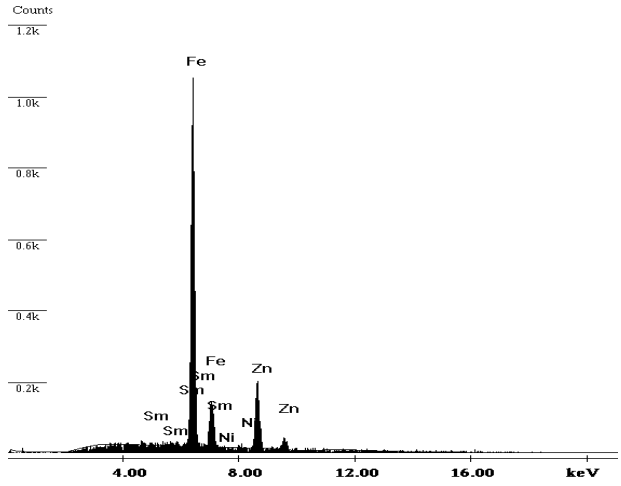

Fig.10 EDX pattern for $Zn_{1-x-y}Ni_ySm_xFe_2O_4$ x=0.01 y=0.001

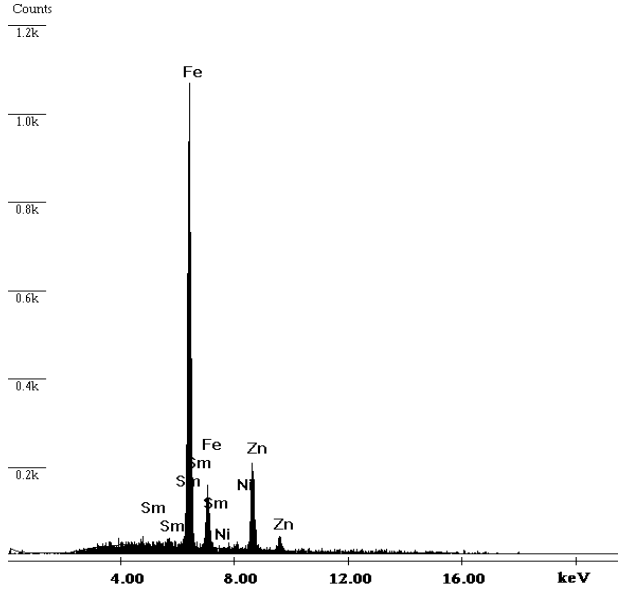

Fig.11 EDX pattern for $Zn_{1-x-y}Ni_ySm_xFe_2O_4$ x=0.012 y=0.001

5. CONCLUSION

From the above experimental results, it is clearly evident that the nano size of the ferrite particles has caused increase in magnetization in Sm doped $ZnFe_2O_4$. Since Saturation magnetization and coercive force increases with the increase in Sm, these parameters will be very useful for the application of the ferrite materials in the antenna construction. This change will be also suitable for reducing the size of the antenna.

6. ACKNOWLEDGEMENTS

One of the authors Dr.VasantNaidu, would like to thank Dr.V.R.K.Murthy, Professor, IIT Madras for his valuable suggestions. Author Dr.VasantNaidu wishes to thank the Dr. S. Sankaran, Director and Dr. Chandra PrakashDRDO,NewDelhi and Dr.S. Pandian, Scientist 'F' DMRL, Hyderabad.

7. REFERENCES:

[1] E.J.W. Verwey, E.L. Heilmann, J. Chem. Phys. 15 1947) 174.

[2] S.M. Yunus, J.A. Fernandez-Baca, M.A. Asgar, F.U. Ahmed, M.A. Hakim, Physica. B+C 262 (1999) 112.

[3] G. Chandrasekaran, P. Nimy Sebastian, Mater. Lett. 37 (1998) 17.

[4] G.Chandrasekaran, S. Selvanandan, K. Manivannane, J. Mater. Sci. 15 (2004) 15.

[5] Pradeep, C.Thangasamy, G. Chandrasekaran, J. Mater. Sci. 15 (2004).

[6] JiZhenxingYue, Li Zhou, Longtu, Hongguo Zhang, ZhilunGui, J. Magn.Magn. Mater. 208 (2000) 55.

[7] ZhenxingYue, WenyuGuo, Ji Zhou, ZhilunGui, Li Longtu, J. Magn.Magn. Mater. 270 (2004) 216.

[8] P Hayley Spiers, Ivan. Parkin, A Quentin. Pankhurst,LouiseAffleck,Mark Green, J Daren. C V aruana, Maxim. Kuznetsov, Jun Yao, Gavin Vaughan, Ann Terry, AkeKvick, J. Mater. Chem. 14 (2004) 1104.

[9] G.M Bhongale., D.K Kulkarni., V.B Sapre., Bull, Mater.Sci.15 (1992)121.

[10] A Pradeep.,P Priyadharsini., GChandrasekaran., Journal of MagnMag.Mater, 320 (2008) 2779.

[11] L. Ne´el, J. Phys. Rad. 17 (1956) 250.

[12] B.K. Labde, C. Madan Sable, N.R. Shamkuwar, Mater. Lett. 57 (2003) 1651.

[13] G.M. Bhongale, D.K. Kulkarni, V.B. Sapre, Bull. Mater. Sci. 15 (1992)121.

[14] R.D. Waldron, Phys. Rev. 99 (6) (1955) 1727.

[15] S.A. Patil, ,et.al, Solid State Commun. 78(1)(1991) 39.

[16] H Sato., T Umeda.. et,.al, Synthesis of Magnetic Glass Ceramics Based on Strontium .vol.34, no. 1, (1993) pp. 76–81.

[17] F Cheng.,,et.al., Microstructure, magnetic and magneto-optical Properties of chemical synthesized Co-RE (RE = Ho, Er, Tm, Yb, Lu) ferrite nanocrystalline films, J. Appl. Phys., 1999, 86 (5): 2727.

[18] L.A Vermenko., T.Y Gridasova., and E.N Lukachina., The effect of addition of rare earth element oxides on the properties of nickel ferrite, Poroshk. Metall., 1973, 9 (129): 52.

[19] N Rezlescu., ERezlescu., C Pasnicu., and M.L Craus., Effect of the rare-earth ions on some properties of nickel-zinc ferrite, J. Phys. Condens. Matter, 1994, 6: 5707.